PROBLEMATIC SIDE VIEWS OF *EPROLITHUS* : COMPARISON WITH *MICULA DECUSSATA*

Davide Persico & Giuliana Villa

Dipt. di Scienze della Terra, Parco Area delle Scienze 157, 43100 Parma, Italy; dotgeo03@nemo.cce.unipr.it; Giuliana.Villa@unipr.it

Key words: Upper Cretaceous, taxonomy, biostratigraphy, *Eprolithus*, *Micula*, nannoliths

Abstract: The morphologies of *Eprolithus floralis*, *Eprolithus octopetalus* and *Eprolithus eptapetalus* have been studied by means of LM/SEM micrographs of the same specimens, as well as via biometric measurements. Interference figures of side-views of certain *Eprolithus* species, which make them appear similar to *Micula decussata*, are shown to be side-views of *E. eptapetalus* and *E. octopetalus*, in which the X represents four elements under the same plane of focus.

Introduction

In this work, we examine in detail the morphologic and structural features of some species belonging to the Family Polycyclolithaceae (Forchheimer, 1972 emend. Varol, 1992), in particular *Eprolithus floralis*, *Eprolithus octopetalus*, *Eprolithus eptapetalus* and *Micula decussata*. Hĕrein, we do not use the name *Micula staurophora* because, as pointed out by Perch-Nielsen (1985), *Discoaster staurophorus* Gardet, 1955 was described from Miocene strata and the holotype was poorly illustrated. For this reason, it is here considered to be invalid for this Cretaceous form and *M. decussata* is used instead. In addition, we use *E. eptapetalus* instead of *Eprolithus moratus* because we believe they are different species. Our examination of the holotypes appears to reveal that the elements of *moratus* twist slightly, whilst they do not appear to in *eptapetalus*, and that the central area is narrower in *moratus* than in *eptapetalus*.

The stratigraphic ranges of the above-mentioned species are fairly well defined, and there is general agreement on their distribution (see Figure 1). Nevertheless, the *M. decussata* first occurrence datum (FO), which is generally placed in the Coniacian at the base of zone CC14 (Sissingh, 1977) or UC10 (Burnett, 1998) (Perch-Nielsen, 1985; Bralower, 1988; Varol, 1992; Burnett, 1998; Bralower & Bergen, 1998; Bergen & Sikora, 1999; Luciani & Cobianchi, 1999), has also been reported from the Early Turonian (Thierstein, 1976; Ghisletti & Erba *in* Premoli Silva & Sliter, 1995).

Thierstein (1976) considered '*Tetralithus pyramidus*' Gardet, 1955 to be a synonym of *M. staurophora* (= *M. decussata*), consequently extending the range of the latter species down into the Early Turonian. Due to the poorly-detailed drawing of the holotype of '*T. pyramidus*', Prins & Perch-Nielsen (*in* Manivit *et al.*, 1977) renamed it *Quadrum gartneri*, the FO of which is in the Early Turonian. Thus, the apparent discrepancy shown by Thierstein (1976) in the earliest occurrence of *M. decussata* is taxonomic, not biostratigraphic.

Apart from the confused synonymy of *M. decussata*, a morphological problem could be the cause of the apparent biostratigraphical discrepancy. In the light-microscope (LM), side-views of *E. octopetalus* and *E. eptapetalus* - a rectangular outline crossed by an X - are reminiscent of *M. decussata*, and this interference figure may have been erroneously interpreted as *M. decussata*. The side-view of *E. floralis* under the LM has an 'H'-shape, as reported in the original description (Stradner, 1962), and cannot easily be confused with *M. decussata*.

The Polycyclolithaceae contain those taxa which possess two superimposed cycles of elements, visible in side-view. The number of elements in each cycle can vary from 3 to *c.*20. This is a fundamental taxonomic feature (for taxonomic remarks, see Appendix and Varol, 1992). In side-view, SEM images of *E. floralis*, *E. octopetalus* and *E. eptapetalus* show two cycles of elements, arranged one on top of another, to form a double 'crown' (Plate 1, Figure 7). In the LM, side-views of *E. octopetalus* and *E. eptapetalus* show an 'X' that is the result of viewing four elements under the same plane of focus, a similar interference figure to that of *M. decussata*.

M. decussata has a cubic shape, composed of eight equal-sized, pyramid-shaped blocks. In the LM, any face of the cube appears to have the same aspect - a square surmounted by a cross, in which the four 'arms' (sutures) are disposed along the diagonals of the square.

Here, we aim to elucidate the structural and morphological features responsible for the optical interference figures that make side-views of *E. octopetalus* and *E. eptapetalus* appear similar to *M. decussata*. This will help to clarify a taxonomic problem which could lead to misinterpretation of the biostratigraphy. This study has also allowed us to overcome such misinterpretation in the LM, during routine analyses, by illustrating that the two genera can be distinguished using the gypsum plate (1λ).

Material and methods

Samples utilised for this work come, in part, from a section of the Basal Complex of the Helminthoid Flysch (Northern Apennines), which is represented by Cenomanian-Turonian turbidite sandstones (Cassolo section: Villa & Persico, 2002). The finding of forms very much like *Micula decussata*, but associated with older species such as *Eprolithus eptapetalus* and *E. octopetalus*, led us to focus on the morphology and structure of the two genera. Samples from ODP Leg 171, Hole 1050C, cores 20-21, in

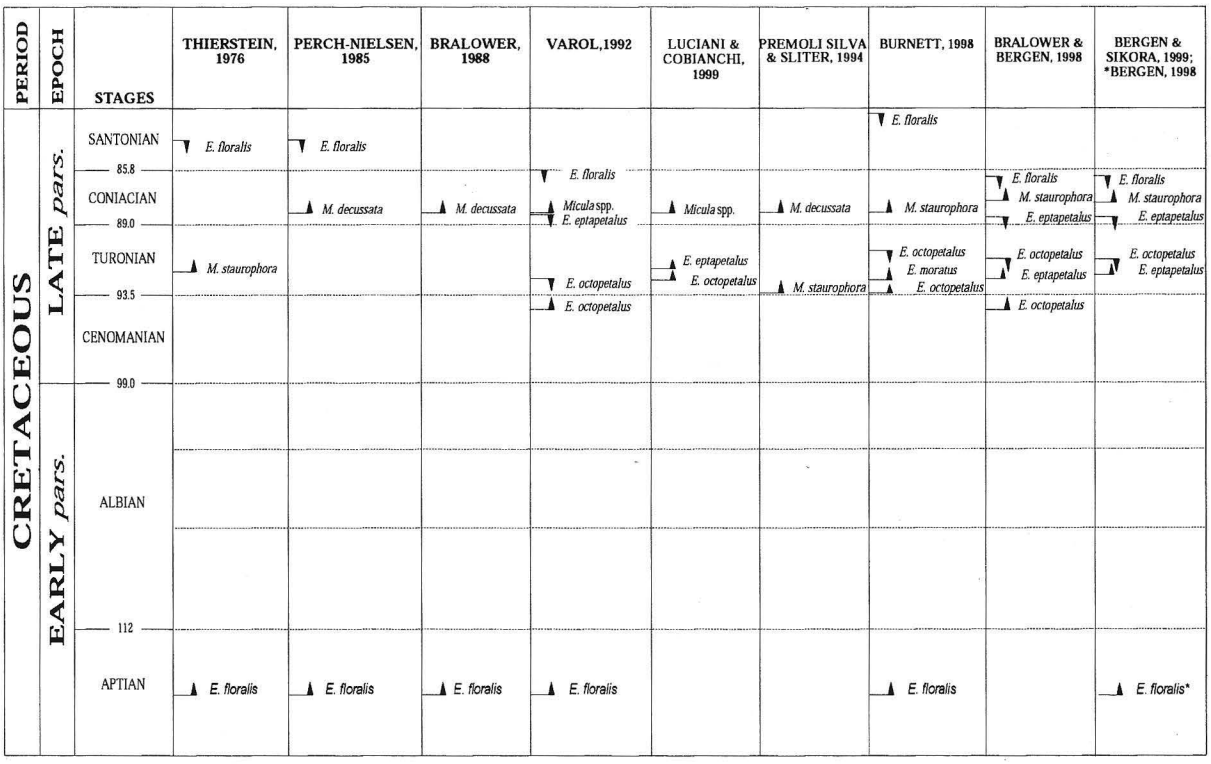

Figure 1: Stratigraphic positions of the first and last occurrences of the discussed species, according to different authors. The positioning of the *E. octopetalus* and *E. eptapetalus* first and last occurrences exhibit slight differences between the authors. The FO of *M. decussata* (= *M. staurophora*) shows major diachronism.

which good nannofossil preservation allowed useful SEM analysis, were also studied.

Eprolithus was never abundant in this material, and so the samples were prepared using a concentration technique (de Kaenel & Villa, 1996). Parameters used to differentiate between *Eprolithus* species included number of wall elements, maximum diameter of the nannolith, and diameter of the central area.

To determine with more confidence if the 'X'-shaped side-view forms (XSVF) observed in the LM belonged to *E. eptapetalus* and *E. octopetalus* or to *M. decussata,* we observed the same fossil specimens both in LM and SEM, using the methodology described in Moshkovitz (1977). This technique confirmed that the postulated *M. decussata*s were, in fact, side-views of *E. eptapetalus* and *E. octopetalus* (Plate 1, Figures 3-4). To support this simple observation, several biometric measurements were performed in the LM, in order to obtain the mean of the maximum diameter (D), the central-area diameter (d), and the length (L) (Figure 2) of about 30 randomly-chosen specimens.

For the biometric analyses, samples with good preservation were selected, recovered from different, known stratigraphic levels from the Cenomanian, Coniacian and Santonian. This excluded any overlapping of the biostratigraphic ranges of the two genera under examination and, thus, avoided taxonomical mistakes.

Results

The main results obtained from the biometric measurements can be summarised as follows:

1. The measurement of d and D in 30 specimens of *Eprolithus floralis, E. octopetalus* and *E. eptapetalus* in plan-view allowed the evaluation of the ratio D/d, in order to obtain an absolute value, independent from the size of each specimen, which indicated the size of the central area (Figure 3).

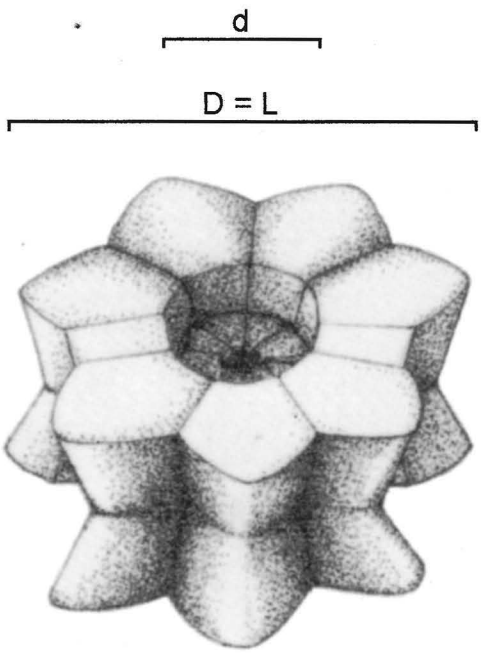

Figure 2: Biometric parameters of measurements on *Eprolithus*. The maximum diameter (D) of *Eprolithus* in plan-view corresponds to the length (L) of *Eprolithus* in side-view.

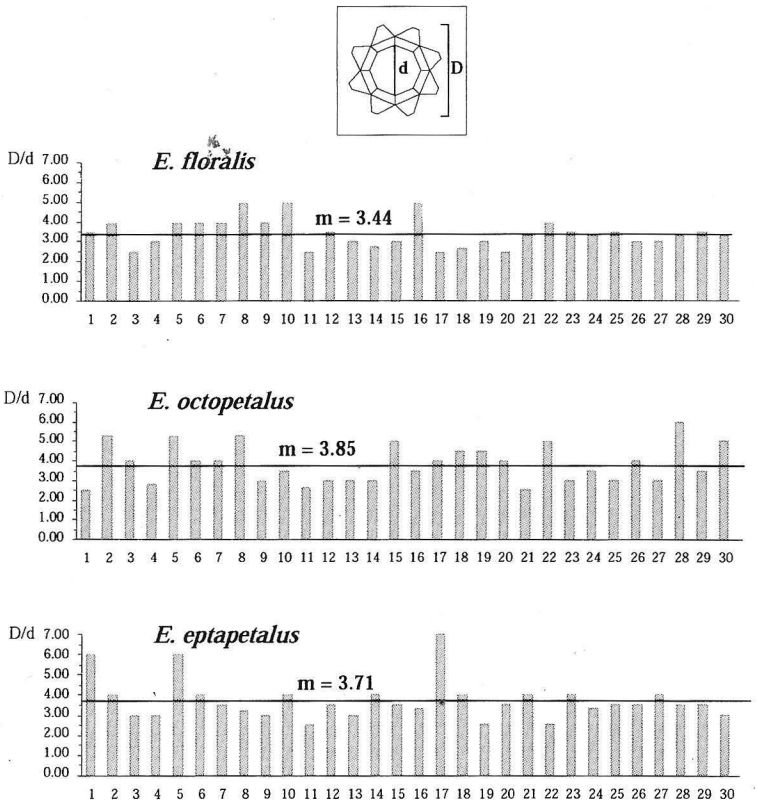

Figure 3: Histograms of size distribution (LM) of 30 specimens of *E. floralis*, *E. eptapetalus* and *E. octopetalus*. D is the outer diameter, d is the central-area diameter, m indicates the mean. The D/d ratio gives an indication of the central-area dimensions.

face of 30 specimens of *M. decussata* was measured (Figure 4, bottom right). The resulting mean is 5.06μm, which excludes a correspondence of *M. decussata* with the XSVF, which were larger.

Now that it can be demonstrated that SEM-illustrated distinctions between the taxa are supported by the LM-based biometric measurements, it is also useful to provide a tool for use in distinguishing the optical behaviour of the side-views of *E. eptapetalus* and *E. octopetalus* from views of *M. decussata*, which could be used during routine LM analysis, especially when dealing with samples that are not in stratigraphic order. With the gypsum plate, *M. decussata* assumes a typical colour alternation (blue-yellow: Moshkovitz & Osmond, 1989) of the four 'arms' of the 'X' on each face of the cube (Plate 2, Figures 10, 12). This pattern is not so evident in the *Eprolithus* side-views, in which the colours vanish from the centre toward the wall (Plate 2, Figures 6, 8). In addition, in the LM, when focusing on a side-view of *Eprolithus*, all the elements of the wall become gradually visible (Figure 5), an aspect that cannot be present in *M. decussata*, because its eight elements make up a cube.

2. In the Cenomanian sample (ODP 1050C-21R-3, 56cm) (Huber *et al.*, 1999), only 'H'-shaped side-view forms (HSVF) were observed, belonging to *E. floralis* (as described in Stradner's (1962) original description). Biometric measurements of plan-views of 30 specimens of *E. floralis* revealed a maximum diameter (D) ranging from 4 to 8μm (mean 5.85μm) (Figure 4, top left). In another 30 specimens of HSVF, the length measurement (L) ranged from 4 to 7μm (mean 5.16μm) (Figure 4, top right). This good biometric correspondence confirms that L and D are the same parameter, and that all the measured forms belonged to the same species.

3. In the Turonian sample (ODP 1050C-21R-1, 59-60cm) (Huber *et al.*, 1999), both HSVF and XSVF were observed: the three recorded species of *Eprolithus* are present. The maximum diameter (D) of 30 specimens of *E. octopetalus* and 30 of *E. eptapetalus* were measured, their mean values being 6.76 and 6.63μm, respectively (Figure 4, centre and bottom left). In the same sample, the lengths (L) of 30 XSVF were measured, and the resulting mean value (6.5μm) corresponds well with the above-mentioned mean value of D, confirming the equivalence of either *E. octopetalus* or *E. eptapetalus* with the XSVF (Figure 4, centre right).

4. *M. decussata* is the only representative of the Polycyclolithaceae in the examined Santonian sample (N.13, Cassolo section). The length (L) of the cube

Conclusions

The results allow us to conclude the following:

1. *Eprolithus floralis* has a relative wider central-area than *E. eptapetalus* and *E. octopetalus*, both of which have central-areas of similar size (Figure 3). The shape of the side-view is strictly connected to the central-area size. In fact, large central-area specimens have an 'H'-shaped aspect in side view, as a result of the distance between the wall elements. Small central-area specimens assume, in side-view, the aspect of an 'X', as the elements are close to each other.

2. The 'H'-shaped forms correspond to side-views of *E. floralis* specimens (Figure 4; Plate 2, Figures 13-16).

3. The 'X'-shaped forms with an L mean value of 6.5μm correspond to specimens of *E. eptapetalus* and/or *E. octopetalus*, with a D mean value of 6.76μm and 6.63μm, respectively (Figure 4).

4. The good correspondence between the mean values of D (Figure 4, left column) of the three *Eprolithus* species with the L mean values of HSVF and XSVF (Figure 4, centre and top right) excludes a relationship between *Eprolithus* and *Micula*, the latter having a smaller L mean value.

Through this work, it has been clarified how forms, which in the LM could be confused with *M. decussata*, are actually side-views of *E. eptapetalus* and *E. octopetalus*,

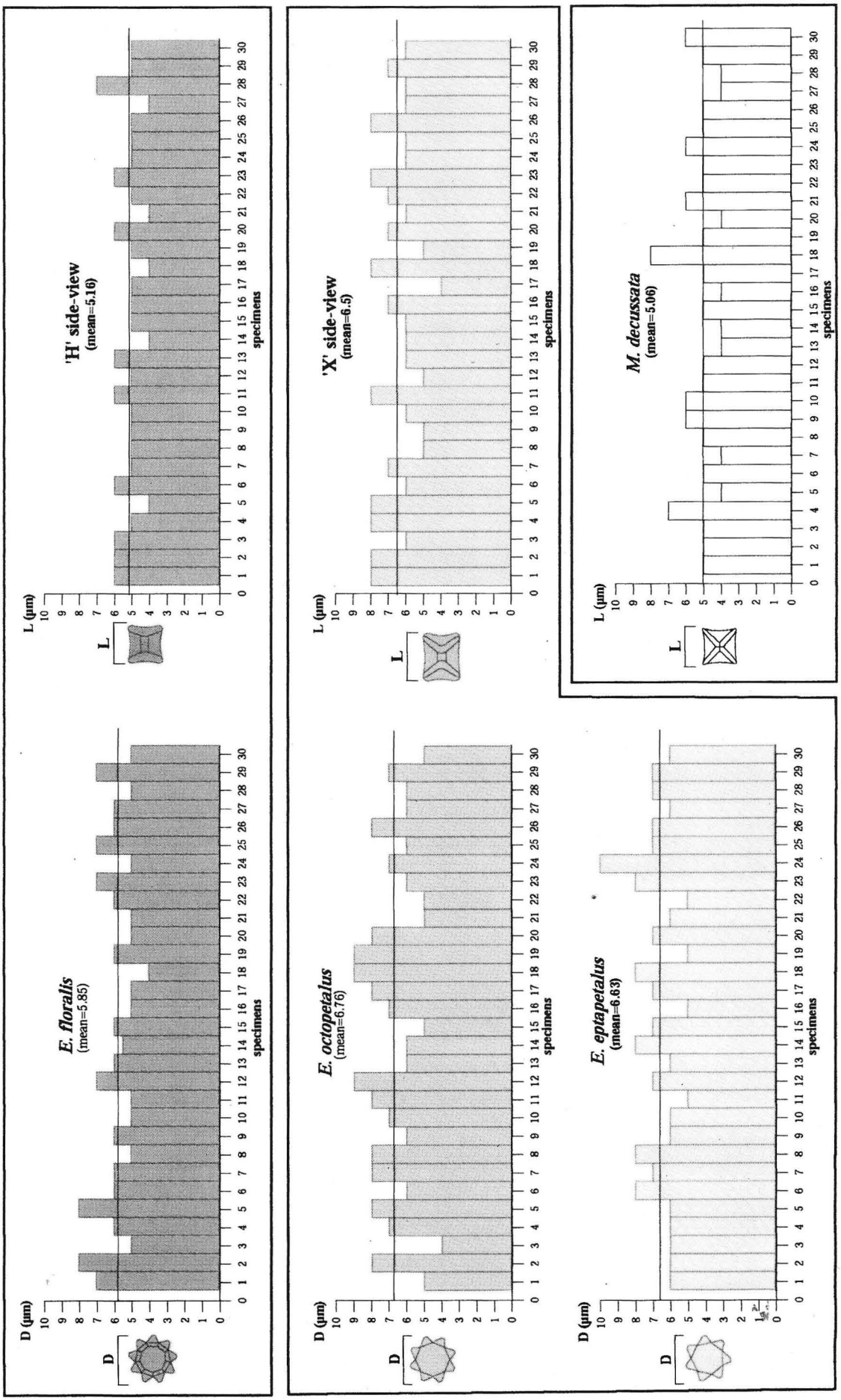

Figure 4: *Left*: histograms showing the distribution of LM-measured diameter (D) of 30 specimens of *E. floralis, E. eptapetalus* and *E. octopetalus*. *Right*: histograms showing the distribution of LM-measured length (L) of 30 specimens with 'H'-shaped and 'X'-shaped side-views, compared with measurements of 30 specimens of *M. decussata*.

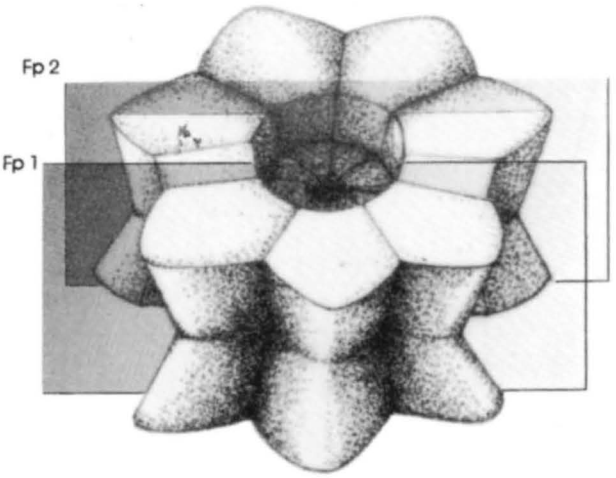

Figure 5: Progressive focal planes (fp) visible in *Eprolithus* species, a feature not observable in *Micula* species.

in which the 'X' is the result of viewing four elements in the same plane of focus. This has been demonstrated by LM/SEM photomicrographs of the same specimens, as well as by biometric measurements. It has also been suggested that these species can be easily distinguished in the LM, with the use of the gypsum plate to detect optical and structural differences. It is thus hoped that this study provides a key to avoiding erroneous classification which can lead to incorrect biochronostratigraphic attributions.

Acknowledgements

This research was derived from a 'Laurea' thesis by the senior author at the University of Parma (Persico, 1998). The first version of the paper benefited from the valuable suggestions of Eric de Kaenel and Miriam Cobianchi, and the final version from the reviewers, Jackie Lees, Jean Self-Trail and Richard Howe. We are grateful to Edvige Masini for her skill and patience in drawing the nannofossils. ODP Leg 171-1050C samples were kindly provided by Brian Huber, Smithsonian Institution.

References

Bergen, J.A. 1998. Calcareous nannofossils from the lower Aptian historical stratotype at Cassis-La Bédoule (SE France). *Géologie Mediterranéenne*, **25**: 227-255.

Bergen, J.A. & Sikora, P.J. 1999. Microfossil diachronism in southern Norwegian North Sea chalks: Valhall and Hod fields. *In*: R.W. Jones & M.D. Simmons (Eds). *Biostratigraphy in Production and Development Geology. Geological Society, London, Special Publication*, **152**: 85-111.

Bralower, T.J. 1988. Calcareous nannofossil biostratigraphy and assemblage of the Cenomanian-Turonian boundary interval: implication for the origin and timing of oceanic anoxia. *Paleoceanography*, **3**: 275-316.

Bralower, T.J. & Bergen, J.A. 1998. Cenomanian-Santonian calcareous nannofossil biostratigraphy of a transect across the Western Interior Seaway. *In*: W.E. Dean & M.A. Arthur (Eds). *Stratigraphy and Paleoenvironments of the Cretaceous Western Interior Seaway, USA. SEPM, Concepts in Sedimentology and Paleontology*, **6**.

Bukry, D. 1969. Upper Cretaceous coccoliths from Texas and Europe. *Univ. Kansas Paleontol. Contrib.*, **51** (Protista 2), 1-79.

Burnett, J.A. 1998. Upper Cretaceous. *In*: P.R. Bown (Ed.). *Calcareous Nannofossil Biostratigraphy*. British Micropal. Society Series, Chapman & Hall/Kluwer Academic: 132-199.

Burnett, J.A. 1997. New taxa and new combinations of Cretaceous nannofossils. *Journal of Nannoplankton Research*, **19**: 133-146.

Crux, J.A. 1982. Upper Cretaceous (Cenomanian to Campanian) Calcareous Nannofossils. *In*: A.R. Lord (Ed.). *A Stratigraphical Index of Calcareous Nannofossils*. British Micropal. Society Series, Ellis Horwood Limited, Chichester: 81-135.

Forchheimer, S. 1972. Scanning electron microscope studies of Cretaceous coccoliths from the Köpingsberg Borehole No. 1, SE Sweden. *Sveriges Geologiska Undersokning*, Series C, #668, **65**: 1-141.

Gardet, M. 1955. Contribution à l'ètude des coccolithes des terrains Mesogènes de l'Algérie. *Publ. Serv. Carte Géol. Algerie, Ser. 2*, **5**: 477-550.

Huber, B.T., Leckie, R.M., Norris, R.D., Bralower, T.J. & CoBabe, E. 1999. Foraminiferal assemblage and stable isotopic change across the Cenomanian-Turonian boundary in the subtropical North Atlantic. *Journal of Foraminiferal Research*, **29**: 392-417.

de Kaenel, E. & Villa, G. 1996. Oligocene/Miocene calcareous nannofossil biostratigraphy and paleoecology from the Iberia Abyssal Plain, Northeastern Atlantic. *Proc. ODP Sci. Res.*, **149**: 79-145.

Luciani, V. & Cobianchi, M. 1999. The Bonarelli Level and other black shales in the Cenomanian-Turonian of the northeastern Dolomites (Italy): calcareous nannofossil and foraminifera data. *Cret. Res.*, **20**: 135-167.

Manivit, H., Perch-Nielsen K., Prins, B. & Verbeek, J.W. 1977. Mid-Cretaceous calcareous nannofossil biostratigraphy. *Koninklijke Nederlandse Akademie van Wetenschappen*, **B80**(3): 169-81.

Moshkovitz, S. 1978. New types of cover slip and mounting slide with a graticule for examination of the same small object by the light microscope and the scanning electron microscope. *Microscopica Acta*, **80**: 161-166.

Moshkovitz, S. & Osmond, K. 1989. The optical properties and microcrystallography of Arkhangelskiellaceae and some other calcareous nannofossils in the Late Cretaceous. *In*: J.A. Crux & S. van Heck (Eds). *Nannofossils and their applications. Proceedings of the INA Conference, London, 1987*: 76-97.

Perch-Nielsen, K. 1985. Mesozoic calcareous nannofossils. *In*: H.M. Bolli, J.B. Saunders & K. Perch-Nielsen (Eds). *Plankton Stratigraphy*. Cambridge University Press, Cambridge: 329-426.

Persico, D. 1998. *Biostratigrafia a nannofossili calcarei delle Arenarie di Ostia e Scabiazza, Appennino Settentrionale (Prov. di Parma e Piacenza)*. Unpubl. thesis.

Premoli Silva, I. & Sliter, W.V. 1995. Cretaceous planktonic foraminiferal biostratigraphy and evolutionary trends from the Bottaccione section, Gubbio, Italy. *Paleontographia Italica*, **82**: 1-89.

Sissingh, W. 1977. Biostratigraphy of Cretaceous calcareous nannoplankton. *Geol. Mijnbouw*, **56**: 37-65.

Stover, L.E. 1966. Cretaceous coccoliths and associated nannofossils from France and Netherlands. *Micropaleontology*, **12**: 133-167.

Stradner, H. 1962. Uber neue und wenig bekannte Nannofossilien aus Kreide und Alttertiar. *Sonderabdrukaus den Verhandlungen der geologischen Bundesanstalt*, **2**: 363-377.

Stradner, H. 1963. New contributions to Mesozoic stratigraphy by means of nannofossils. *Proceedings of the Sixth World Petroleum Congress,* **Section 1, Paper 4**: 167- 184.

Thierstein, H.R. 1976. Mesozoic calcareous nannoplankton biostratigraphy of marine sediments. *Marine Micropaleontology*, **1**: 325-362.

Varol, O. 1992. Taxonomic revision of the Polycyclolithaceae and its contribution to Cretaceous biostratigraphy. *Newsletters on Stratigraphy*, **27**: 93-127.

Vekshina, V.N. 1959. Coccolithophoridae of the Maastrichtian deposits of the west Siberian lowlands. *SNIIGGIMS*, **2**: 56-77.

Villa, G. & Persico, D. 2002. Calcareous nannofossil biostratigraphy of the Ostia and Scabiazza Sandstones (Val Trebbia, Val Ceno, Val Taro, Northern Apennines): a key to a Cretaceous tectono-stratigraphic interpretation. *Mem. Soc. Geol. It.*

Appendix: Systematic palaeontology

Genus: *Micula* Vekshina, 1959

Type species: *Micula decussata* Vekshina, 1959

Micula decussata Vekshina, 1959
Plate 1, Figures 5, 8; Plate 2, Figures 9-12

1955 *Discoaster staurophorus* Gardet: 534, pl.10, fig.96.
1959 *Micula decussata* Vekshina: 71-72, pl.1, fig.6; pl.2, fig.11.
1963 *Micula staurophora* (Gardet) Stradner *partim.*: 174, pl.4, fig.12a; *non* pl.4, figs 12, 12b, 12c.
1969 *Micula decussata* Vekshina: Bukry, 67, pl.40, figs 5-6.
1976 *Micula staurophora* (Gardet) Stradner: Thierstein *partim.*, 352, pl.1, fig.9; pl.4, figs 34-35; *non* pl.1, fig.10.
1985 *Micula decussata* Vekshina: Perch-Nielsen, 390-391, figs 58.6-58.12, 58.28.
1998 *Micula staurophora* (Gardet) Stradner: Burnett, 194, pl.6.13, fig.25.

Remarks: A short taxonomic note on *M. decussata* is reported in the text, above. Essentially, Thierstein's (1976, p.352) confusion of '*Tetralithus pyramidus*' (= *Quadrum gartneri*) with *M. staurophora* meant that his FO for *M. staurophora* was erroneously low. *Micula* and *Quadrum* are quite distinct genera: *Micula* can be easily distinguished from *Quadrum* with the use of the gypsum plate, as *Micula* spp. (with the exception of *Micula murus*) assume the typical blue/yellow alternation pattern, opposite to that of *Quadrum* spp., which display the yellow/blue crystallographic direction (Moshkovitz & Osmond, 1989).
Dimensions: Holotype 3μm; studied samples 5μm.
Range: Early Coniacian - Late Maastrichtian.

Genus *Eprolithus* Stover, 1966

Type species: *Lithastrinus floralis* Stradner, 1962

Remarks: *Eprolithus* differs from other polycycloliths by having petal-like elements making up the wall/rim. The wall/rim is composed of two cycles of elements, and the number of elements is a species-level taxonomical character.

Eprolithus floralis (Stradner) Stover, 1966
Plate 2, Figures 4, 13-16

1962 *Lithastrinus floralis* Stradner, *partim.*: 370, 372, pl.2 figs 7, 9-11; *non* pl.2, figs 6, 8.
1966 *Eprolithus floralis* (Stradner) Stover: 149, pl.7, figs 4-7, 9; pl.9, fig.21.
1998 *Eprolithus floralis* (Stradner) Stover: Burnett, 192, pl.6.13, figs 3a-b.

Remarks: A species of *Eprolithus* having nine petal-like elements in each cycle of the wall/rim. In side-view, it assumes an 'H' aspect. It is worth noting that also *Radiolithus* spp. in side-view show an 'H' aspect, however, in *Radiolithus* the 'H' appears stretched, with a wider 'bridge' (the diaphragm), and the wall/rim height is lower than that of *Eprolithus*.
Dimensions: Holotype 8-10μm; studied samples 5.85μm.
Range: Middle Aptian – Late Coniacian. Burnett (1998) reports a Middle Aptian-?Campanian range.

Eprolithus eptapetalus Varol, 1992
Plate 1, Figures 1, 7; Plate 2, Figures 1-2

1978 *Lithastrinus grillii* Stradner: Proto-Decima *et al.*, pl.16, figs 1a-c.
1992 *Eprolithus eptapetalus* Varol: 104, pl.1, figs 2-4; pl.6, figs 8-13.
1998 *Eprolithus moratus* (Stover) Burnett: 192, pl.6.13, figs 5a-6.

Remarks: An *Eprolithus* having seven petal-like elements, radially inclined, in each cycle of the wall.
Dimensions: Holotype 7-11μm; studied samples 6.63μm.
Range: Early Turonian – Early Coniacian.

Eprolithus octopetalus Varol, 1992
Plate 1, Figure 2; Plate 2, Figure 3

1992 *Eprolithus octopetalus* Varol: 104, pl.1, figs 5-10; pl.6, figs 14-15.
1998 *Eprolithus octopetalus* Varol: Burnett, 192, pl.6.13, figs 4a-b.

Remarks: *Eprolithus* with eight petal-like elements in each cycle. In side-view, it is indistinguishable from *E. moratus.*
Dimensions: Holotype maximum diameter 5.0μm; studied samples 6.76μm.
Range: Late Cenomanian – Middle Turonian.

Plate 1

All photomicrographs were taken with a digital camera, the files are stored on a CD in the Dept. of Earth Science, University of Parma

Fig.1: *E. eptapetalus*, XPL and SEM (plan-view). ODP Hole 1050C-21R-1, 59-60cm.
Fig.2: *E. octopetalus*, XPL and SEM (side-view). ODP Hole 1050C-21R-1, 59-60cm.
Fig.3: *Eprolithus* sp., same specimen, XPL and SEM (side-view). ODP Hole 1050C-21R-1, 59-60cm.
Fig.4: *Eprolithus* sp., same specimen, XPL and SEM (side-view). ODP Hole 1050C-21R-1, 59-60cm.
Fig.5: *M. decussata*, XPL and SEM (plan-view). N.13 Cassolo section.
Fig.6: *M. concava*, XPL and SEM (side-view). N.13 Cassolo section.
Fig.7: *E. eptapetalus* line-drawings and SEM (side-view). ODP Hole 1050C-21R-1, 59-60cm.
Fig.8: *M. decussata* line-drawings and SEM (side-view). ODP Hole 1050C-21R-1, 59-60cm.

Plate 1

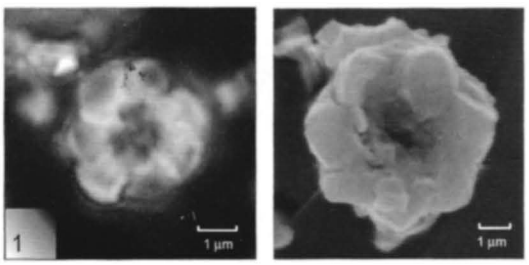

E. eptapetalus

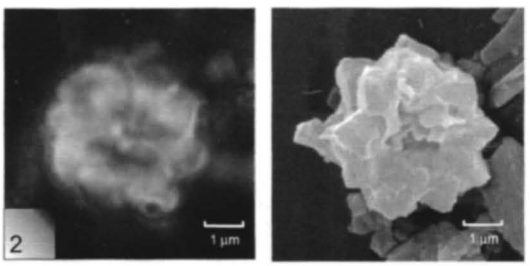

E. octopetalus

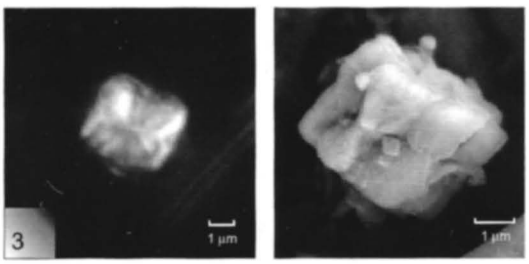

Eprolithus sp.

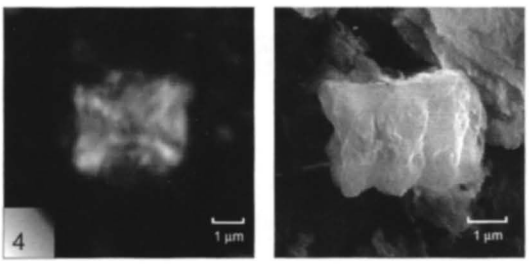

Eprolithus sp.

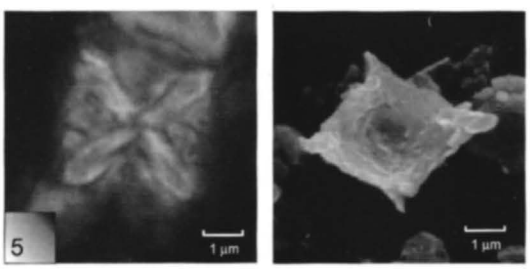

M. decussata

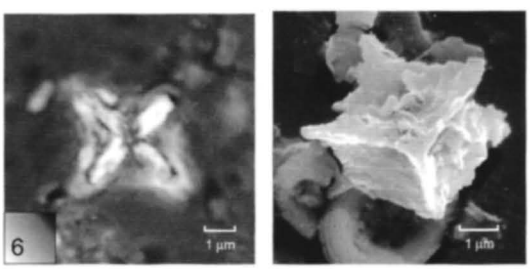

M. concava

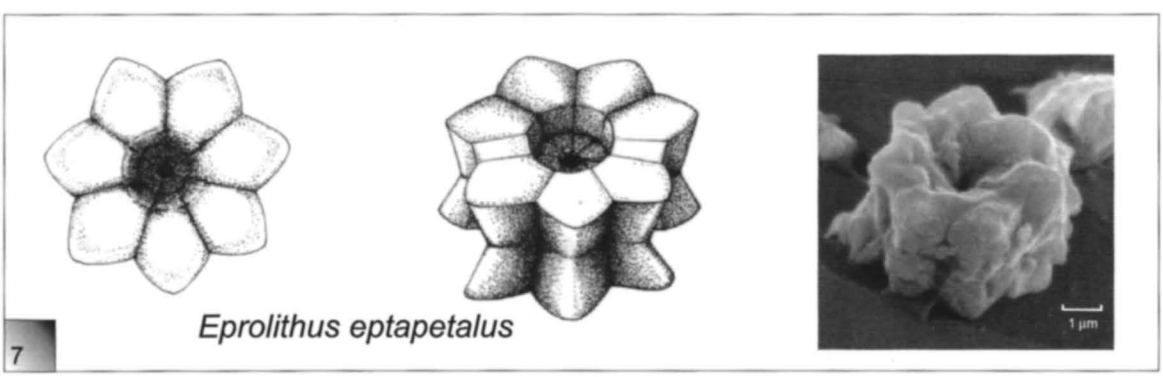

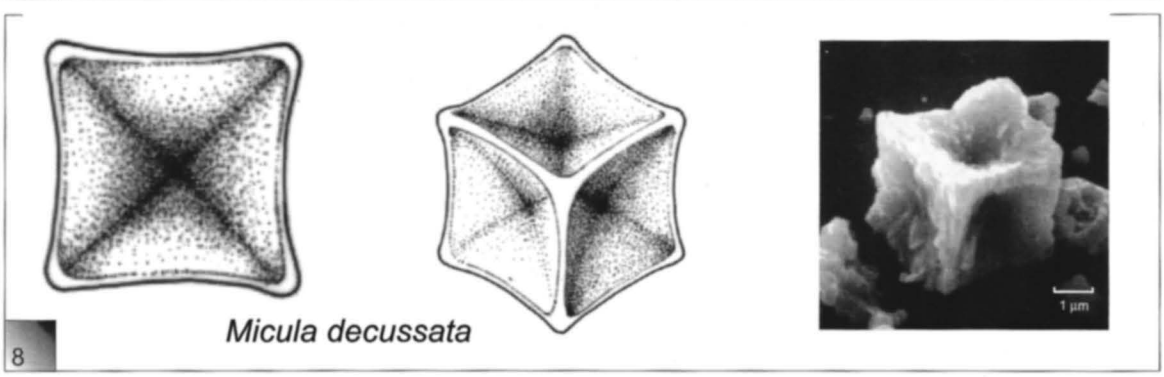

Plate 2

Figs 1-2: *Eprolithus eptapetalus*, XPL. ODP Hole 1050C-21R-1, 59-60cm.
Fig.3: *Eprolithus octopetalus*, XPL. ODP Hole 1050C-21R-1, 59-60cm.
Fig.4: *Eprolithus floralis*, XPL. ODP Hole1050C-21R-1, 59-60cm.
Figs 5-6: *Eprolithus* sp. ('X' side-view), XPL, gypsum plate. ODP Hole1050C-21R-1, 59-60cm.
Figs 7-8: *Eprolithus* sp. ('X' side-view), XPL, gypsum plate. ODP Hole1050C-21R-1, 59-60cm.
Figs 9-10: *Micula decussata*, XPL, gypsum plate. N.13 Cassolo section.
Figs 11-12: *M. decussata*, XPL, gypsum plate. N.13 Cassolo section.
Figs 13-14: *E. floralis* ('H' side-view), XPL, gypsum plate. ODP Hole1050C-21R-3, 56-59cm.
Figs 15-16: *E. floralis* ('H' side-view), XPL, gypsum plate. ODP Hole 1050C-21R-3, 56-59cm.

Plate 2

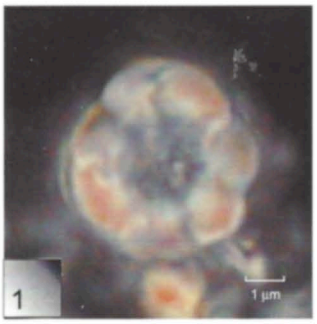

E. eptapetalus

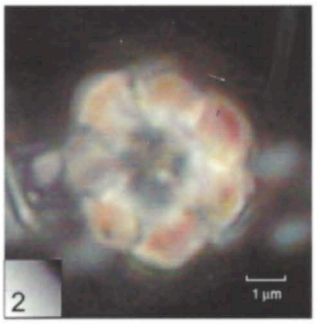

E. eptapetalus

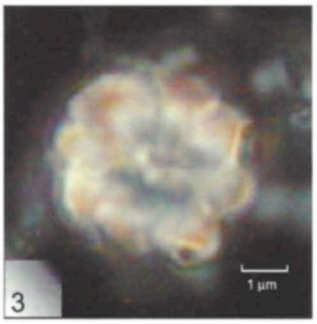

E. octopetalus

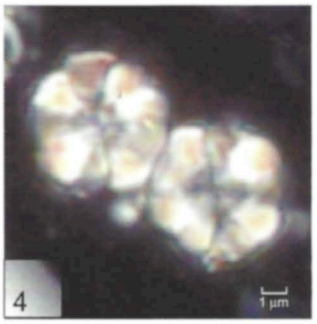

E. floralis

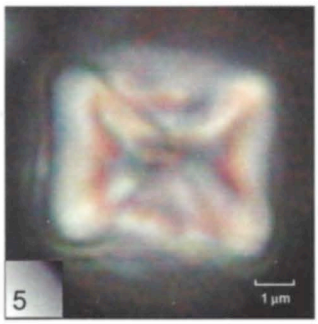

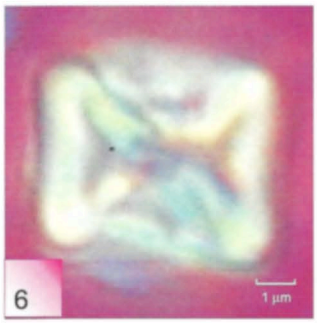

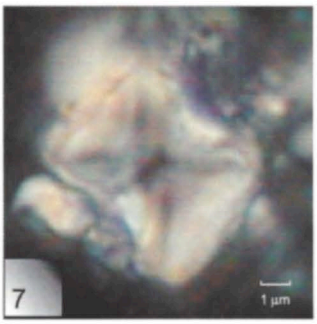

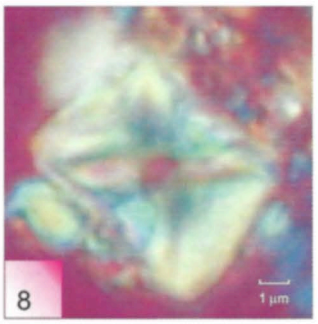

Eprolithus sp. "X" side view

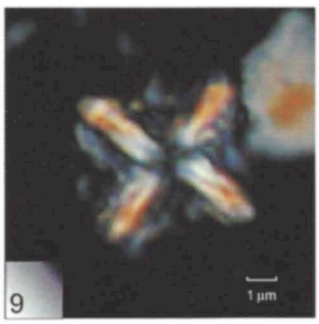

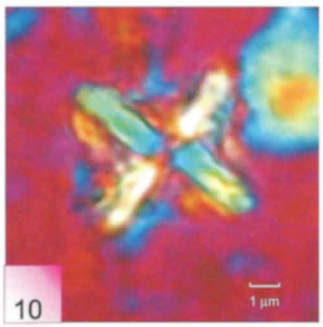

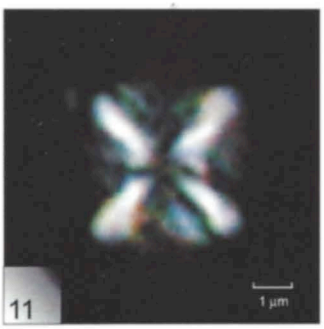

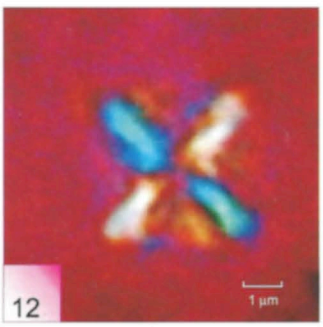

M. decussata

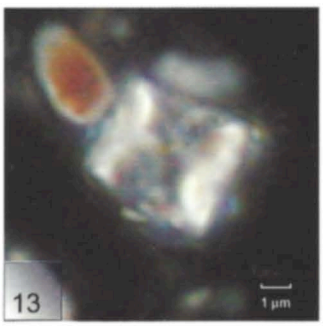

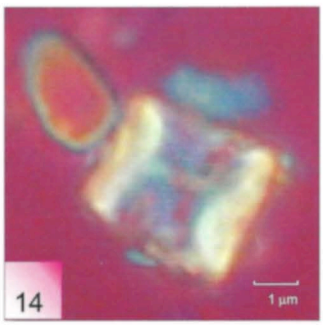

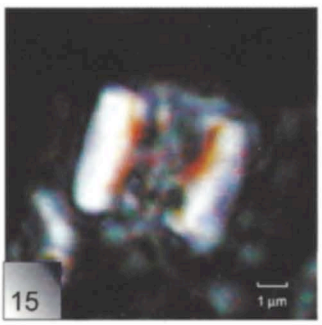

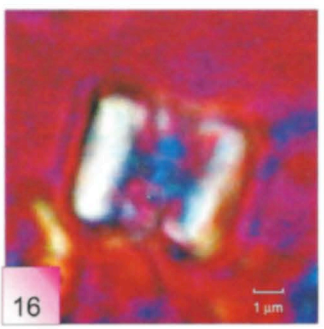

E. floralis: "H" side view